Hydrothermal synthesis of MnO_2@graphene/activated carbon composite electrode with enhanced electrochemical performance for supercapacitor applications

Manoranjan Mandal[1], Subhasri Subudhi[1], Injamul Alam[1], BVRS Subramanyam[1], Santosini Patra[1] and Pitamber Mahanandia[1]*

[1]*Department of Physics & Astronomy, National Institute of Technology, Rourkela-769008*

Email: pitam@nitrkl.ac.in

Abstract

We report the preparation of an electrode material made up of MnO_2/ graphene/ activated carbon ternary composite by hydrothermal method for supercapacitor (SC) applications. The prepared ternary composite has been characterized by using scanning electron microscopy (SEM), powder X-ray diffraction (XRD), energy dispersive spectroscopy (EDS) and Raman spectroscopy measurements. The prepared objective electrode has been investigated using galvanostatic charge-discharge (GCD) and cyclic voltammetry (CV) measurements in a 3-electrode system using 3M KOH aqueous electrolyte for the analysis of their electrochemical performance. The prepared MnO_2/graphene/activated carbon composite results in maximum capacitance of ~ 493.57 F/g at 5 mV/s using CV and moreover the highest capacitance obtained from the GCD measurement is ~ 485.29 F/g at 1 A/g. The long-term cycle stability of the composite electrode is also demonstrated and it shows outstanding cyclic performance where 97% of capacitance is left over 5000 cycles at 1 A/g. Therefore, the composite shows good charge storage performance, as well as tremendous cycle stability and that, reveal the synthesized ternary composite can be a suitable electrode for SC applications.

Keywords: *Activated carbon, graphene, galvanostatic charge-discharge, MnO_2, cyclic voltammetry*

1. Introduction

During the decades, a crucial amount of effort has been given to develop high energy storage and conversion device owing to the growing demands for power systems. Supercapacitors (SCs) are the novel class of storage device having high power density (20-30 times) compare to conventional batteries and more energy density than the commercial dielectric capacitors [1-4]. Due to their fast charging-discharging capabilities, long cycle life (> 100000 cycles), high output power supply in a short time and simple operation process, SC has applications in many fields including hybrid electric vehicles, memory back-up systems, consumer electronics and industrial power supplies [5]. However, low energy density and very fast discharging of SCs limits its applications in many energy-demanding fields. Therefore, most researchers in this field have given special attention to enrich the energy performance of SCs short of losing their power performance and cycle

life. There are various kind of electrode materials such as the different form of carbon (activated carbon, graphene, carbon nanotube etc.), conductive polymers and transition metal oxides have been extensively investigated to get the enhanced energy and power density in SCs [6-15]. Among various carbon materials, activated carbon (AC) has attracted much for SCs application as electrode material owing to its large specific surface area, high packing density and cost-effective. However, less electrical conductivity and lack of mesoporosity result in a smaller specific capacitance and power performance of SC devices based on AC electrode. Therefore, to be used in high-performance SCs, it is essential to achieve good electrical conductivity and developed mesoporosity without losing its surface area.

Owing to its good electrical conductivity, high specific surface area and developed porous structure, graphene (GR) a two-dimensional flexible material has given special consideration for SCs application. Therefore, the drawbacks of AC could be overcome by incorporating graphene. Chao Zheng et al. have synthesized the nanoscale hybrids of GR/AC as an electrode for SCs and found maximum specific capacitance exhibited by GR/AC was 103 F/g and 210 F/g in organic and aqueous electrolytes [16]. Yao Chen et al. have prepared GR/AC composite by chemical activation with KOH and found specific capacitance of composite were 122 F/g in an aqueous electrolyte [17]. Further, the storage performance (capacitance) of carbon-based SC could be enhanced by introducing metal oxides [18-21]. There are various kind of pseudocapacitive metal oxides such as NiO, RuO_2 and MnO_2 [22-24] have been extensively studied as an electrode material for SCs because of their richer in reversible redox reaction at electrode surface results in more specific capacitance than carbon-based electrode materials. Among them, MnO_2 has been considered as a potential candidate to be used in SCs due to its environmental friendliness, high theoretical specific capacitance, low cost and high electrochemical activity [25, 26]. However, the power performance of SCs device based on MnO_2 is very poor due to the low electrical conductivity and hence cannot be used intrinsically. The electrical conductivity of MnO_2 could be improved to a large extend by integrating with conducting substrates such as carbon materials (carbon nanotube, GR and AC). Yue Li et al. have prepared MnO_2 coated on reduced graphene oxide/AC by hydrothermal process and the maximum specific capacitance achieved by the reduced graphene oxide/AC/MnO_2 composite was 378 F/g in 7M KOH solution [27]. Zhuangjun Fan et al. have reported very high energy density and power density by fabricating asymmetric supercapacitor based on GR/MnO_2 and AC nanofibers [28]. They have found the energy density exhibited by the composite was 51.1 Wh/kg and the power density was 198 kW/kg in 1M Na_2SO_4 electrolytic solution.

Based on the above survey, herein we have synthesized MnO_2 nanorods coated on GR/AC as a composite electrode by a simple as well as a low-cost method and achieved the superior capacitance in 3M KOH aqueous electrolyte. The improved electrical conductivity of AC could be achieved by introducing GR in it and at the same time the restacking of GR layers can be evaded by making AC as a separator in between the layers which will result in both the outer portion and inner portion of GR layers can be available to access the electrolyte ions. The addition of MnO_2 nanorods on GR/AC could enhance the specific capacitance by involving reversible redox reaction and simultaneously the conductivity of MnO_2 could be increased due to the presence of GR which might increases the overall storage performance and cycle stability.

2. Experimental

2.1 Chemicals

The reagents have been procured commercially and used without any further purification. The used reagents such as nitric acid, oxalic acid and two high-quality graphite rods have been used.

2.2 Synthesis of MnO_2/graphene/AC composite

Commercially available MnO_2 nanorods and AC have been used here (Sigma-Aldrich (India) company). MnO_2 has been used without doing any further purification and AC was further treated with nitric acid to increase its porosity for better ions accumulation as per the standard procedure [29]. The electrochemical method has been used to synthesize a few layers of graphene sheets (GR) [30] where the interaction between high-quality graphite rods and oxalic acid take place. Good quality of GR was recovered after sonicating and filtering several times. MnO_2/GR/AC composite has been prepared by the process of hydrothermal synthesis. Initially, AC, graphene and MnO_2 are taken with an optimized weight ratio of 1:1:4 (MnO_2: GR: AC) and sonicated individually for 2 hours using 20 ml of ethanol as a solvent. Then the products were mixed and further sonicated for 1 hour to get better dispersion. After sonication, the products are stirred magnetically for 12 hours at room temperature. Then the mixture was kept in a Teflon-line autoclave (100 mL) for 15 hours at 180^0C. The final MnO_2/GR/AC composite was recovered by drying at 100^0C for 24 hours in an air oven.

2.3 Electrodes fabrication for electrochemical measurements

The working electrode is fabricated by mixing Nafion (binder), carbon black and MnO_2/GR/AC composite with a weight ratio of 1:1:8 (to form a slurry). Then 1mg of the slurry was pressed on Ni-foam (10mm ×10mm× 1mm) and dried in a vacuum for 24 hours at 70^0C to form the final electrode. Then the fabricated composite electrode was investigated by GCD and CV measurements in 3M KOH solution in 3 electrode cell where the final fabricated electrode is taken as working electrode, for counter electrode platinum wire is used and Ag/ AgCl as a reference electrode.

3. Results and discussions

The phase purity and crystalline structure of as-synthesized MnO_2/GR/AC composite and precursors have been investigated by using XRD as shown in Fig. 1 (a). AC shows two peaks with (002) and (101) plane confirms the presence of graphite crystalline. GR shows a very sharp and intense peak at $2\theta = 26.77^0$ with (002) plane reveals into the formation of GR and further, confirms the hexagonal structure. MnO_2 nanorods shows strong peaks at $2\theta = 28.63^0$, 37.27^0, 40.93^0, 42.77^0, 46.03^0, 56.62^0, 59.32^0, 64.81^0 and 67.17^0 with (110), (101), (200), (111), (210), (211), (220), (002) and (310) planes corresponds to JCPDS data No. 65-2821 with the tetragonal structure. The reflection peaks are sharper and narrow which indicates MnO_2 nanorods are highly crystallite. When GR and MnO_2 nanorods are added to host AC, two planes (002) and (101) with lower intensity have been found including all the planes of MnO_2 nanorods which confirms the presence of GR and MnO_2 in the composite.

Fig. 1 (b) shows the Raman spectra of prepared MnO_2/GR/AC composite where the degree of graphitization and further formation of the composite are investigated. Two characteristic peaks i.e. D (defects) peak at 1344 cm^{-1} and G (graphite) peak at 1602 cm^{-1} have been found for AC. Similarly, GR shows D and G peaks at 1358 cm^{-1} and 1589 cm^{-1}. Two peaks at 645 cm^{-1} with high intensity and 348 cm^{-1} with less intensity have been found for MnO_2 nanorods which reveal a certain amount of disorder, movements of the individual atoms and also suggest the formation of MnO_2 nanorods. GR/AC composite shows two peaks at 1338 cm^{-1}

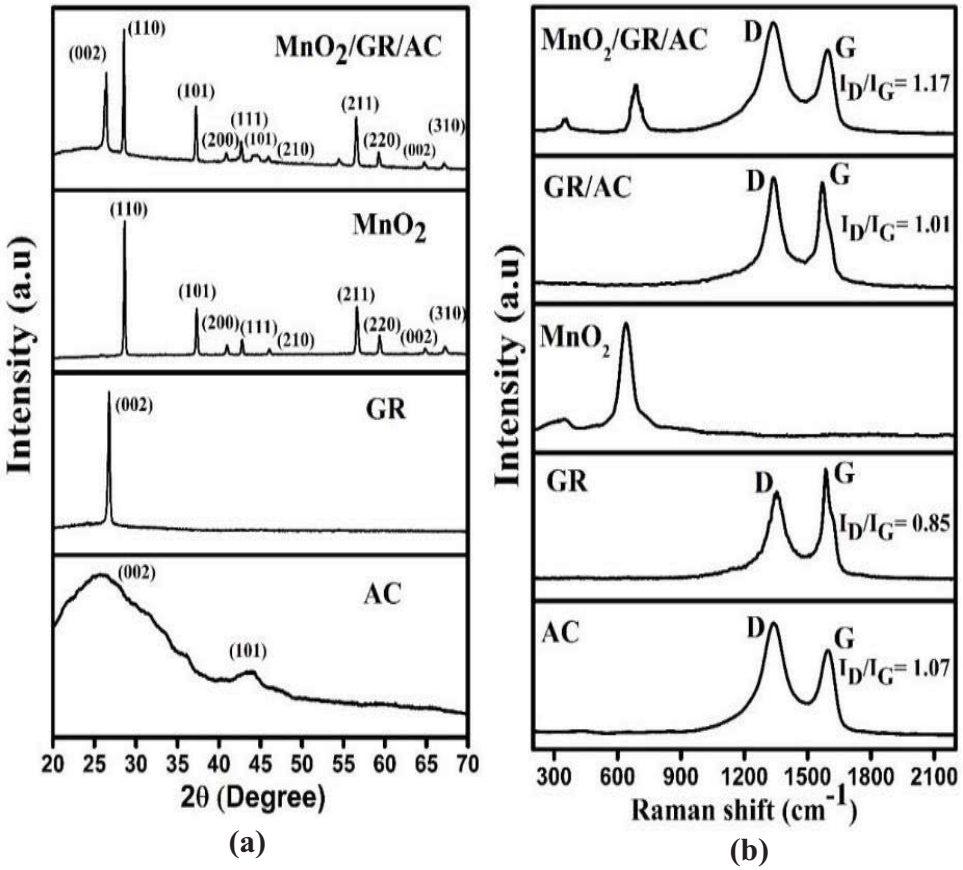

FIG 1. (a) XRD pattern of AC, GR, MnO_2 and MnO_2/GR/AC; (b) Raman images of AC, GR, MnO_2, GR/AC and MnO_2/GR/AC.

and 1569 cm^{-1}. MnO_2/GR/AC composite shows peaks at 1338 cm^{-1}, 1602 cm^{-1} (for both AC and GR), 354 cm^{1} and 684 cm^{-1} (for MnO_2) which reveals the shifting of individual atoms in MnO_2 towards the right and also the presence of MnO_2 in GR/AC composite is confirmed.

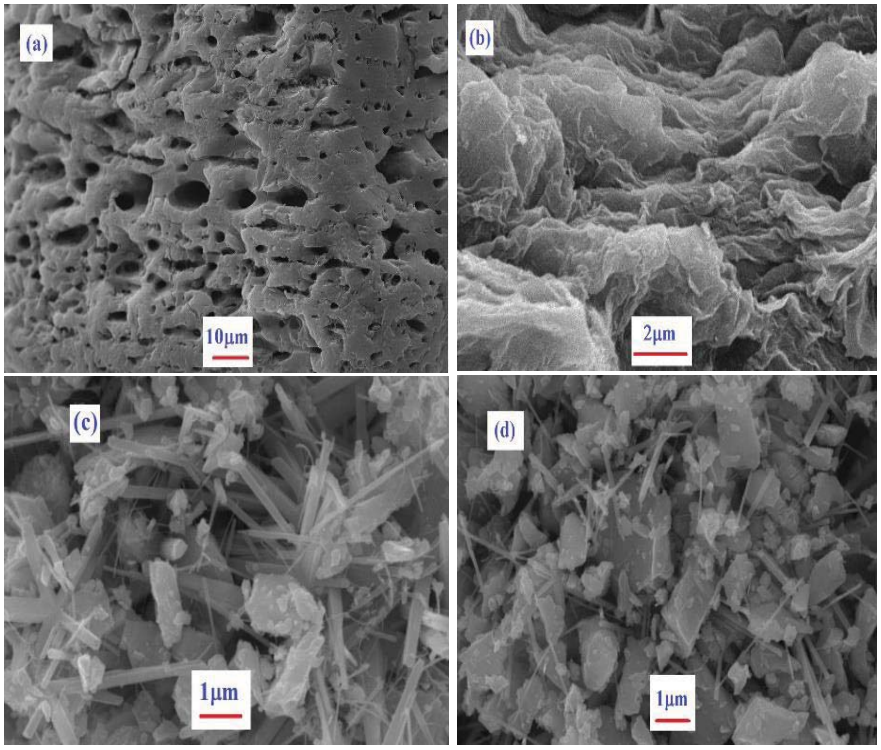

FIG 2. SEM image of (a) AC, (b) GR, (c) MnO_2 nanorods and (d) MnO_2/GR/AC composite.

The microstructure of synthesized MnO_2/GR/AC and precursors is characterized by using SEM which is shown in Fig. 2. The large numbers of pores of AC that accumulate the electrolyte ions at the electrode surface is shown in Fig. 2(a) and the pores are well developed with interconnected to each other. Fig. 2(b) shows the microstructure of GR where the layers are well exfoliated with oriented randomly and also some agglomeration of GR layers have been found. The surface morphology of MnO_2 nanorods is shown in Fig. 2(c) and it is to be noticed that the nanorods have a sharp tip with small in diameter which can be called 'nanoneedles' and also observed that some MnO_2 nanorods are formed like layer structure. The presence of GR and MnO_2 nanorods on host AC are well observed in Fig. 2(d) where GR and the MnO_2 nanorods are uniformly distributed over AC. Further using EDS analysis, the presence of MnO_2 nanorods and GR in host AC has been confirmed.

Fig. 3 shows the presence of chemical compositions in prepared MnO_2/GR/AC composite which was investigated by using EDS. The peaks are clearly showing as C (carbon), Mn (manganese) and O (oxygen). The peak 'C' confirms the presence of both GR and AC. The peaks of 'Mn' and 'O' responds to MnO_2 nanorods in MnO_2/GR/AC composite.

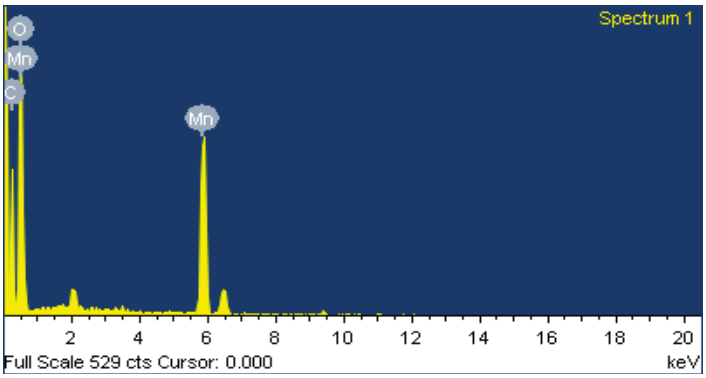

FIG 3. EDS plot of prepared MnO_2/GR/AC composite.

The fabricated composite electrode and precursors (MnO_2, GR and AC) are investigated by using CV and GCD measurements to quantify their storage performance and cycle stability. The specific capacitance was calculated using Eq. (1) (from CV measurement) and Eq. (2) (from GCD measurement) for the fabricated electrodes as follows:

$$C_{sp} = \frac{Ai}{2.\Delta V.\frac{dv}{dt}.m} \quad (1)$$

$$C_{sp} = \frac{I.\Delta t}{m.\Delta V} \quad (2)$$

Where C_{sp} is the specific capacitance (F/g), Ai is the total area under the curve for one cycle (AV), ΔV is the potential window (V), m is the loading mass of electrode material (mg), I is the current density (A/g) and $\frac{dv}{dt}$ is the scan rate (mV/s).

Fig. 4 (a) shows the CV curves of MnO_2, GR, AC and MnO_2/GR/AC composite at 5 mV/s in 3M KOH solution where the composite electrode gives the large area under the CV curve compared to the precursors which reveal the good charge storage capacity of prepared MnO_2/GR/AC composite [31]. The carbon materials (GR and AC) shows almost rectangular CV curves as expected to be EDLC behaviour, however, the redox peak is observed for MnO2 as it involves redox reaction. The CV curves of the synthesized composite at different scan rates of 5-100 mV/s within -0.2 to 0.5 V potential ranges are shown in Fig. 4 (b). It has been observed that the total area under the CV curve of composite increases gradually when increasing the scan rates (5 to 100 mV/s) and the shape of the curves does not change with scan rate that result in fast charge transfer within MnO_2/GR/AC electrode [32]. The capacitances of MnO_2/GR/AC electrode were evaluated using Eq. (1) and the capacitances are 493.57, 393.5, 314.28, 245.89, 188.25 and 165.93 F/g at 5, 10, 20, 40, 80 and 100 mV/s.

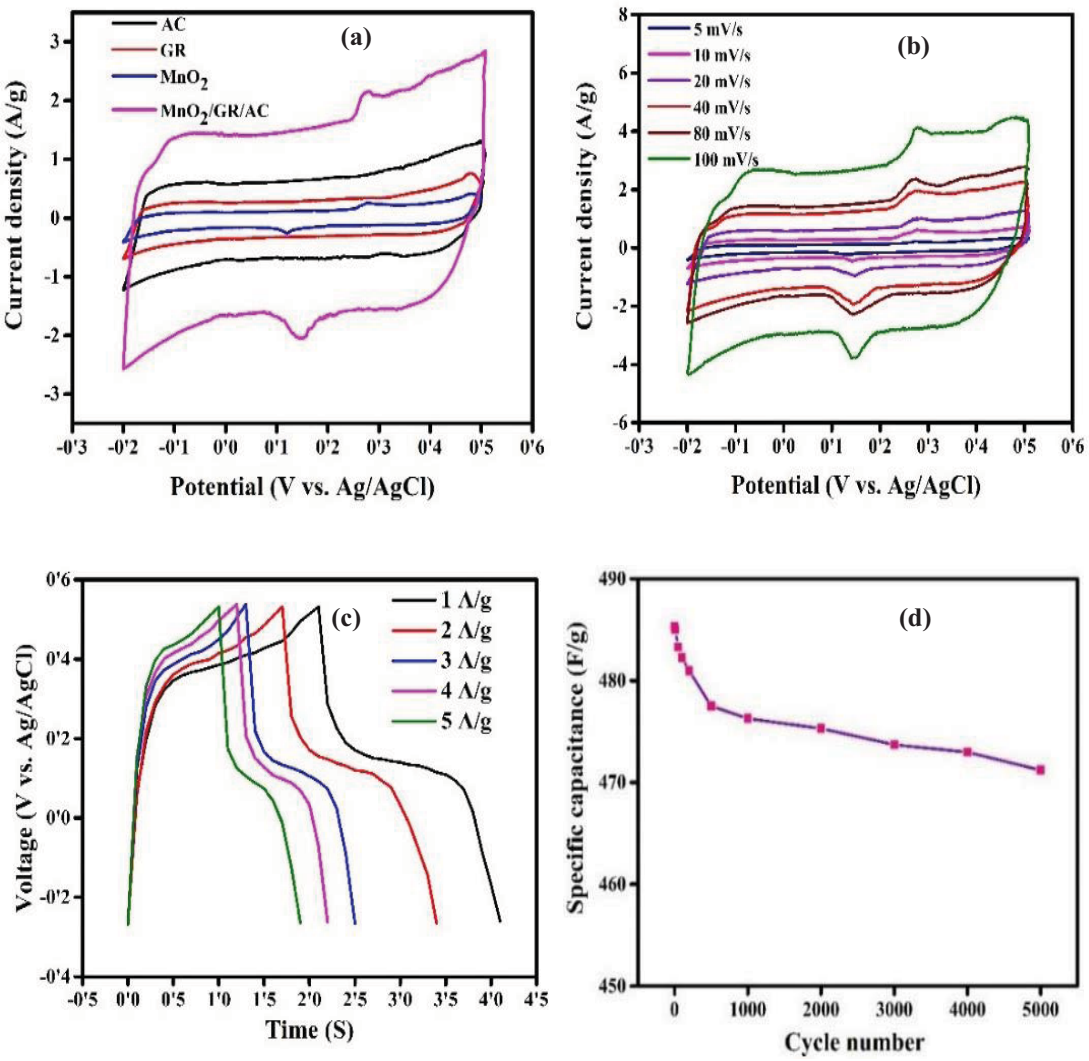

FIG 4. (a) CV plots of AC, GR, MnO_2 and MnO_2/ GR/AC composite (b) CV plots of synthesized MnO_2/ GR/AC composite at different scan rates (c) GCD plots of prepared composite at different current densities and (d) Cyclic performance of composite over 5000 cycles.

The ternary MnO_2/GR/AC has resulted in the utmost capacitance of 493.57 F/g at 5 mV/s and that is significantly more compared to the precursors (AC gives 251 F/g, GR gives 271 F/g, MnO_2 gives 183 F/g). The enormous capacitance in MnO_2/GR/AC because of the presence of highly conducting GR increases the rate of ions transfer within the composite electrode and both surface (lower and upper) of GR able to access the electrolyte ions by making AC as a spacer between the GR layers. Also, the presence of MnO_2 provides a fast reversible redox reaction so that more number of electrolyte ions were accessed by the composite electrode and hence, results in an increase in capacitance of the composite electrode. Fig. 4 (c) shows the GCD curves of the prepared composite at different current densities from 1 to 5 A/g and the curves are

results in non-triangular which disclose the reduction and oxidation reaction is present in between the electrolyte and composite electrode and also confirms the presence of MnO_2. The specific capacitances of composite calculated using Eq. (2) were 485.29, 379.42, 257.63, 248.82 and 153.68 F/g at 1, 2, 3, 4 and 5 A/g. The highest capacitance exhibited by the composite was 485.29 F/g at 1 A/g and the obtained capacitances from GCD are reliable with the CV results which also indicate that the prepared MnO_2/GR/AC composite has excellent storage capacity. Fig. 4 (d) shows the long term cycle stability of the prepared composite and 97% of capacitance is left for 5000 cycles at 1 A/g. Therefore, the composite not only results in improved storage capacity but also outstanding cycle stability.

Fig. 5 (a) shows the deviation in capacitance of MnO_2/GR/AC composite at different scan rates (5-100 mV/s) and the capacitance decreases when increasing the scan rate due to the shortage of time of electrolyte ions to enter the small pores of the composite electrode at high scan rate and that results into lower capacitance [33]. Fig. 5 (b) shows the variation in capacitance of composite at different current densities (1-5 A/g) and observed that the capacitance decreases when increasing the current density probably at high current the limitation of mass transfer occurs (electrolyte ions) at the electrode surface.

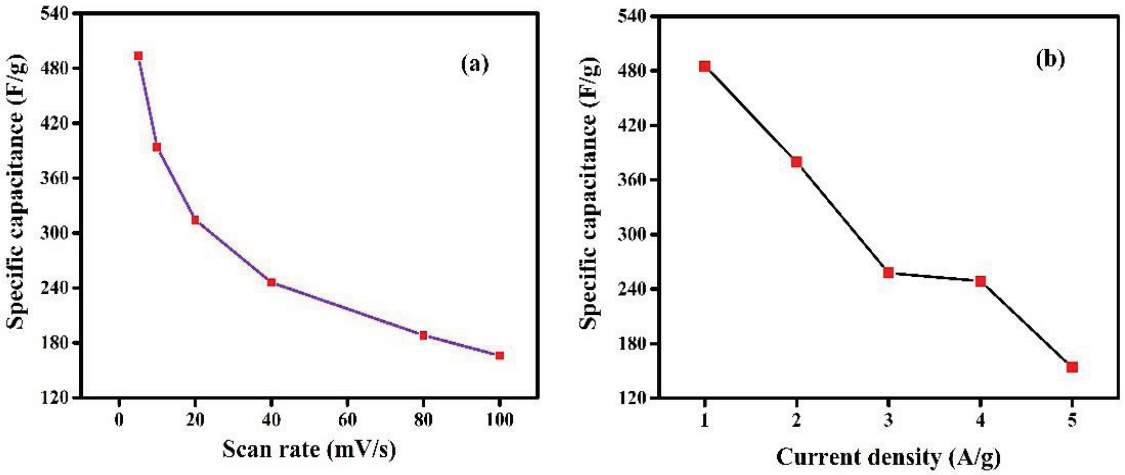

FIG 5. (a) Change in capacitance of synthesized MnO_2/GR/AC composite at different scan rate and (b) specific capacitance of composite at different current density.

4. Conclusions

We have successfully prepared the MnO_2/GR/AC electrode using a cost-effective and simple method. The composite electrode has resulted in a maximum capacitance of 493.57 F/g at 5 mV/s as investigated by using CV and also from GCD measurement, the specific capacitance was found to be 485.29 F/g at 1 A/g. Moreover, the composite gives significantly higher capacitance than the precursors which indicate that the prepared composite has good storage capacity. Long term cycle stability of prepared composite has been investigated and 97% of capacitance has leftover 5000 cycles. Therefore, incorporating MnO_2 and GR in

host AC has shown improved charge storage performance as well as excellent cycle stability and can be considered as an emerging electrode material for the SCs applications.

5. Acknowledgement

I am thankful to the Ministry of Human Resource Development (MHRD) for providing financial support.

REFERENCES

[1] M Winter and R. J Brodd, Chem. Rev. 104, 4245 (2004).

[2] G.W Yang, C.L Xu and H.L Li, Chem. Commun. 48, 6537 (2008).

[3] P Simon and Y Gogotsi, Nat. Mater. 7, 845 (2008).

[4] D Liu, Q Zhang, P Xiao, B.B Garcia, Q Guo, R Champion and G Cao, Chem. Mater. 20, 1376 (2008).

[5] S.H Li, Q.H Liu, L Qi, L.H Lu and H.Y Wang, Chin. J. Anal. Chem. 40, 339 (2012).

[6] C Peng, S Zhang, D Jewell and G. Z Chen, Natural Science 18, 777 (2008).

[7] S.L Chou, J.Z Wang, S.Y Chew, H.K Liu and S.X Dou, Electrochem Commun 10, 1724 (2008).

[8] L. Ci, S. M. Manikoth, X. Li, R. Vajtai and P. M Ajayan, Adv. Mater. 19, 3300 (2007).

[9] C Kim, Y.O Choi, W.J Lee and K.S Yang, Electrochim. Acta 50, 883 (2004).

[10] Y.Y Horng, Y.C Lu, Y.K Hsu, C.C Chen, L.C Chen and K.H Chen, J. Power Sources 195, 4418 (2010).

[11] R.R Bi, X.L Wu, F.F Cao, L.Y Jiang, Y.G Guo and L. J Wan, J. Phys. Chem. C 114, 2448 (2010).

[12] Y Shan and L Gao, Mater. Chem. Phys. 103, 206 (2007).

[13] H.J Choi, S.M Jung, J.M Seo, D.W Chang, L. Dai and J.B Baek, Nano Energy 1, 534 (2012).

[14] M Mandal, S Subudhi, I Alam, B.V.R.S Subramanyam, S Patra, J Raiguru, S Das and P Mahanandia, Inorganic Chemistry Communications 123, 108332 (2021).

[15] M Mandal, S Subudhi, I Alam, B.V.R.S Subramanyam, S Das, J Raiguru and P Mahanandia, AIP Conference Proceedings 2265, 030599 (2020).

[16] C Zheng, X Zhou, H Cao, G Wang and Z Liu, J. Power Sources 258, 290 (2014).

[17] Y Chen, X Zhang, H Zhang, X Sun, D Zhang and Y Ma, RSC Adv. 2, 7747 (2012).

[18] K Lota, A Sierczynska and G Lota, Int. J. Electrochem. 2011, 321473 (2010).

[19] X.H Xia, J.P Tu, Y.J Mai, R Chen, X.L Wang, C.D Gu and X.B Zhao, Chem.–Eur. J. 17, 10898 (2011).

[20] G.Y He, J.H Li, H.Q Chen, J. Shi, X.Q Sun, S. Chen and X. Wang, Mater. Lett. 82, 61 (2012).

[21] X Meng, L Lu and C Sun, ACS Appl. Mater. Interfaces 10, 16474 (2018).

[22] T Cottineau, M Toupin, T Delahaye, T Brousse and D B_elanger, Appl. Phys. A: Mater. Sci. Process. 82, 599 (2006).

[23] M Toupin, T Brousse and D Belanger, Chem. Mater. 16, 3184 (2004).

[24] D.W Wang, F Li and H.M Cheng, J. Power Sources 185, 1563 (2008).

[25] G Yu, L Hu, M Vosgueritchian, H Wang, X Xie, J.R McDonough, X Cui, Y Cui and Z Bao, Nano Lett. 11, 2905 (2011).

[26] M Toupin, T Brousse and D Bélanger, Chem. Mater. 16, 3184 (2004).

[27] Y Li, L Xu, J Gao and X Jin, RSC Adv. 7, 39024 (2017).

[28] Z Fan, J Yan, T Wei, L Zhi, G Ning, T Li and F Wei, Adv. Funct. Mater. 21, 2366 (2011).

[29] D Satapathy and G.S Natarajan, Indian journal of chemistry 45A, 2011 (2006).

[30] P Mahanandia, F Simon, G Heinrich and K. K Nanda, RSC Chem. Commun. 50 4613 (2014).

[31] S Chen, J Zhu, H Zhou and X Wang, RSC Adv. 1, 484 (2011).

[32] C Zheng, X Zhou, H Cao, G Wang and Z Liu, Journal of Power Sources 258, 290 (2014).

[33] Q Cheng, J Tang, J Ma, H Zhang, N Shinya and L.C Qin, Phys. Chem. Chem. Phys. 13, 17615 (2011).